Hybridization and Melting Behavior of Peptide Nucleic Acid (PNA) Oligonucleotide Chimeras Conjugated to Gold Nanoparticles

by **Deirdre Murphy**[a]), **Gareth Redmond**[a]), **Beatriz G. de la Torre**[b]), and **Ramon Eritja***[b])

[a]) National Microelectronics Research Center (NMRC), Lee Malting, Cork, Ireland
[b]) Department of Molecular Genetics, Institut de Biología Molecular de Barcelona, C.S.I.C., Jordi Girona 18–26, E-08034 Barcelona, Spain
(phone: +34(93)4006145; fax: +34(93)2045904; e-mail: recgma@cid.csic.es)

Peptide nucleic acids (PNA) and PNA–DNA chimeras carrying thiol groups were used for surface functionalization of Au nanoparticles. Conjugation of PNA to citrate-stabilized Au nanoparticles destabilized the nanoparticles causing them to precipitate. Addition of a tail of glutamic acid to the PNA prevented destabilization of the nanoparticles but resulted in loss of interaction with complementary sequences. Importantly, PNA–DNA chimeras gave stable conjugates with Au nanoparticles. The hybridization and melting properties of complexes formed from chimera–nanoparticle conjugates and oligonucleotide–nanoparticle conjugates are described for the first time. Similar to oligonucleotide–nanoparticle conjugates, conjugates with PNA–DNA chimeras gave sharper and more-defined melting profiles than those obtained with unmodified oligonucleotides. In addition, mismatch discrimination was found to be more efficient than with unmodified oligonucleotides.

Introduction. – Oligonucleotide-bearing Au nanoparticles were first described in 1996 [1][2]. These conjugates have been shown to form periodic arrays [1][3][4] and to form predetermined dimeric and trimeric assemblies [2][5]. The special properties of Au nanoparticles linked to oligonucleotides have attracted large interest due to their potential use in gene analysis [6–12].

Peptide nucleic acids (PNA) are oligonucleotide analogues in which the negatively charged sugar-phosphate backbone has been replaced by a neutral backbone of *N*-(2-aminoethyl)glycine units, with the common nucleic acid bases attached *via* a carbonyl methylene linker [13]. PNA Oligomers recognize and bind to a specific DNA or RNA strand with high affinity and selectivity [14][15]. Their chemical stability and their resistance to nucleases and proteases make PNA oligomers good candidates as therapeutic agents, diagnostic tools, and probes in molecular biology [15]. The addition of a PNA part to DNA to form PNA–DNA chimeras results in new structures which have combined properties from PNA and DNA. They show improved aqueous solubility due to the partially negatively charged backbone, and they bind exclusively in the antiparallel orientation as DNA [16].

There is a large interest in the field of DNA derivatives as scaffolds for nanomaterials which have the same recognition properties as natural DNA but which have more stability or hydrophobicity to improve the properties of the conjugates. For example, the functionalization of the ends of single-walled C-nanotubes was successfully achieved only by using PNA derivatives [17]. Conjugation of biotinylated-PNA to streptoavidin/avidin nanoparticles results in formation of new drug derivatives for

antisense therapy [18][19] and improved detection at DNA-functionalized electrodes [20]. Recently, investigations of Au nanoparticles modified with PNA have shown that the PNA moiety can modulate the electrostatic surface properties and control nanoparticle assembly rates and aggregate size [21].

In the present communication, we study the use of PNA and PNA–DNA chimeras for functionalization of the surface of citrate-stabilized Au nanoparticles. We show that the presence of a few negative charges are needed to stabilize the Au nanoparticles in solution and that PNA–DNA chimeras conjugated to Au nanoparticles remain stable after functionalization. The hybridization and melting properties of complexes formed from chimera–nanoparticle conjugates and oligonucleotide–nanoparticle conjugates are explored, and sensitive mismatch discrimination, when the mismatch is located in the DNA part of the chimera, is demonstrated.

Results and Discussion. – 1. *Synthesis of Peptide Nucleic Acids* (PNA) *and PNA–DNA Chimeras Carrying Thiol Groups.* PNA Sequence **1** (*Table 1*) was prepared by sequential addition of the commercially available Boc/Z PNA monomers as described elsewhere [22]. The progress of the coupling reactions was monitored by the ninhydrin test [23]. Cysteine protected with the 4-methoxybenzoyl group was added at the N-terminal position to generate a free thiol group after removal of the protecting groups. The desired sequence was purified by HPLC. The same sequence but carrying three glutamic acid residues at the C-terminal position (sequence **2**, *Table 1*) was prepared in a similar way. In this case, the γ-carboxylic acid group of glutamic acid was protected with the (9*H*-fluoren-9-yl)methyl (Fm) group that was removed with piperidine before the removal of the Z groups at the end of the synthesis.

Table 1. *Peptide Nucleic Acids* (PNA), *PNA–DNA Chimeras, and Oligonucleotide Sequences Prepared in This Work.* Peptide nucleic acids are shown in italics. Ac = acetyl, Cys = cysteine, Glu = glutamic acid, Gly = glycine. Residues involved in mismatch are shown in bold.

	Type	Sequence 5′ → 3′ or N → C
1	PNA	H-Cys-*ATGCTCAACTCT*-$CONH_2$
2	PNA	Ac-Cys-*ATGCTCAACTCT*-GluGluGluGly-$CONH_2$
3	PNA-DNA	Thiol-hexyl-TCGACTA*TGCAT*-CONH-hexyl-OH
4	PNA-DNA MM	Thiol-hexyl-TCGA**G**TA*TGCAT*-CONH-hexyl-OH
5	DNA	Thiol-hexyl-TCGACTATGCAT
6	DNA COMP	Thiol-hexyl-ATGCATAGTCGA
7	DNA MM1	Thiol-hexyl-AT**C**CATAGTCGA
8	DNA MM2	Thiol-hexyl-ATGCATA**C**TCGA
9	DNA control	Thiol-hexyl-GCTGTACAAGTA
10	COMP TO 1	Thiol-hexyl-AGAGTTGAGCAT

The synthesis of PNA–DNA chimeras **3** and **4** were performed by using the methodology described previously [24–27]. In this strategy, the monomethoxytrityl (MeOTr) group is used for the temporary protection of the backbone amino function, and acyl protecting groups are used for the protection of the exocyclic amino functions of the nucleobases [24–27]. The MeOTr is removed under mild conditions (3% CCl_3COOH in CH_2Cl_2), and the nucleobase protecting groups are removed by using concentrated aqueous ammonia. These conditions are similar to those employed in

DNA synthesis, allowing the preparation of molecules carrying both PNA and DNA moieties. The connection of the PNA and the DNA part was done by using a thymine PNA linker molecule carrying an OH protected with the MeOTr group [25][27][28]. The oligonucleotide part was assembled on an automatic DNA synthesizer by means of standard protocols.

2. *Synthesis and Properties of Oligonucleotide – Gold-Nanoparticle Conjugates.* Peptide nucleic acids, PNA – DNA chimeras, and complementary oligonucleotides carrying thiol groups (see **1** – **10** in *Table 1*) were treated with citrate-stabilized Au nanoparticles (13 nm) to obtain Au nanoparticles with several oligonucleotide molecules per nanoparticle [7]. When Au nanoparticles were mixed with the all-PNA sequence **1**, a precipitate was immediately formed, indicating that the PNA molecules occupied the citrate binding sites, and, as a result of the loss of surface negative charge, the nanoparticles were no longer stable in solution. When the reaction was performed with sequence **2** carrying the glutamic acid tail, no precipitation was observed, indicating that the glutamic acid tail prevented destabilization of the nanoparticles. However, when nanoparticles carrying sequence **2** were mixed with nanoparticles carrying the complementary sequence **10**, no hybridization was observed. The expected red-to-blue color change that accompanies hybridization of oligonucleotide – nanoparticle conjugates [1] was not observed, and the resulting solutions did not show any characteristic melting behavior when heated (followed by UV/VIS absorption spectroscopy). By comparison, the duplex formed by the same compounds without nanoparticles gave the expected melting profiles (data not shown), indicating that either surface functionalization of the Au nanoparticles with PNA **2** did not occur, or, if it did occur, then the sequence was not accessible to hybridization. These results are in agreement with previously reported data [21].

Consequently, the use of PNA – DNA chimeras for Au nanoparticle derivatization was explored. Functionalization of citrate-stabilized Au nanoparticles with PNA – DNA chimeras was performed in the same manner as for unmodified oligonucleotides. No aggregation of the conjugates that were formed was observed. The chimera – nanoparticle conjugate **3** and complementary oligonucleotide – nanoparticle conjugate **4** were then mixed together in equimolar amounts in hybridization buffer. During the hybridization process, the solution changed from an initial red color to a pale blue/black color. Oligonucleotide hybridization results in the formation of 3D interlinked networks of nanoparticles. Significant spectral changes, therefore, occur in the UV/VIS absorption spectra of these solutions due to the formation of nanoparticle aggregates following hybridization of the oligonucleotides or chimera-oligonucleotides. These large absorbance changes, as compared with unmodified oligonucleotides, are a result of the marked sensitivity of nanoparticle optical properties (especially the surface plasmon resonance) to the reduced internanoparticle distances that occur when the nanoparticles are brought into close proximity following hybridization [3][4][6 – 8]. The magnitude and reversibility of these spectral changes allows the progress of hybridization and subsequent denaturation to be monitored optically for very small oligonucleotide concentrations.

The melting behavior of the hybridized complex formed from chimera – nanoparticle conjugate **3** and complementary oligonucleotide – nanoparticle conjugate **6** was then studied. UV/VIS Absorption spectra were recorded as a function of increasing

temperature. As the solution temperature increases, the oligonucleotide and chimera strands separate, and, hence, the cross-linked nanoparticles also become separated and redisperse into solution, causing a reversal of the spectral changes that occurred during hybridization [3][4][6–8]. Thus, this melting transition represents the breakdown of the 3D interlinked Au nanoparticle networks following oligonucleotide-chimera complex denaturation. Consequently, the melting profile of the hybridized complex formed from chimera–nanoparticle conjugate **3** and oligonucleotide-nanoparticle conjugate **6**, shown in *Fig. 1*, is distinct and well-defined in comparison with the very poorly resolved melting profile acquired for the identical oligonucleotide-chimera complex formed without nanoparticle tags, also shown in *Fig. 1*.

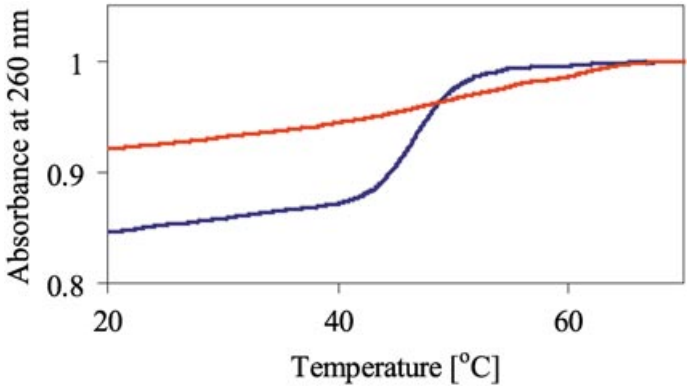

Fig. 1. *Melting profiles at 260 nm of duplexes formed by a PNA–DNA chimera and the complementary DNA sequence.* Duplexes are formed by mixing chimera–nanoparticle conjugate **3** with complementary oligonucleotide–nanoparticle conjugate **6** (blue line) and chimera **3** with oligonucleotide **6** (red line).

An interesting aspect of duplexes that incorporate PNA moieties is the low dependence of duplex stability on ionic strength. This is due to the elimination of the repulsion between phosphate groups in PNA · DNA duplexes. In our case, we employ DNA–PNA chimeras so the duplex will more closely resemble a DNA · DNA duplex. With respect to solution ionic strength, when chimera–nanoparticle conjugate **3** is mixed with complementary oligonucleotide–nanoparticle conjugate **6** in hybridization buffer containing 50 mM or 100 mM NaCl, no color change associated with hybridization was observed, and no melting transitions were observed on heating. This confirmed that a relatively high salt concentration is needed in the buffer to obtain chimera hybridization, as in the case of DNA · DNA duplexes.

The presence of base mismatches in oligonucleotide sequences was also studied. As can be seen from *Fig. 2* and *Table 2*, introduction of one mismatched base into chimera–nanoparticle and oligonucleotide–nanoparticle complexes resulted in the lowering of the melting temperature and the magnitude of the hyperchromic change associated with each melting transition. These effects were more pronounced when the mismatch was incorporated into the DNA part, where no transition at all was observed (duplexes **4** · **6** and **3** · **8**). On the other hand, a mismatch within the PNA part (duplex **3** · **7**) gave the same melting profile as a mismatch within a DNA · DNA duplex (duplex **5** · **7**). It has been reported that mismatch discrimination is higher in PNA derivatives.

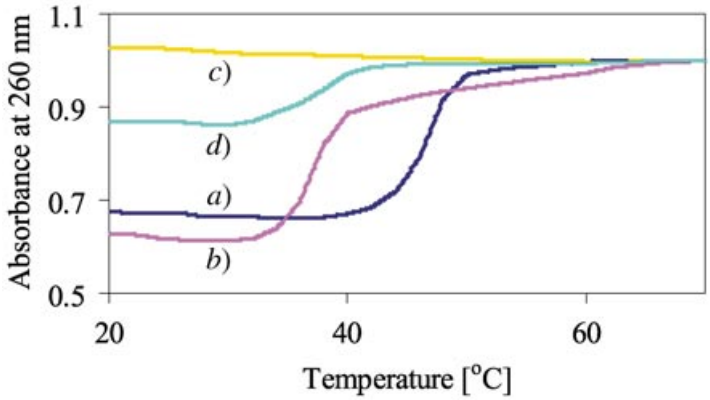

Fig. 2. *Effect of the mismatch on the melting profiles at 260 nm of duplexes formed by PNA–DNA chimeras and their complementary DNA sequences* (both conjugates to Au nanoparticles). a) *DNA · DNA perfect match* **5**–**6**. b) *DNA · Chimera perfect match* **4**·**8**. c) *DNA · Chimera mismatch in DNA part* **3**·**8**. d) *DNA · Chimera mismatch in PNA part* **3**·**7**. Conditions: 0.3M NaCl and 10 mM sodium phosphate pH 7.

Table 2. *Melting Characteristics of Duplexes Linked to Gold Nanoparticles.* Exper. conditions: 0.3M NaCl and 10 mM sodium phosphate pH 7.

	Type of duplex	Duplex	T_m [°]	Hyperchromicity [%]
5·**6**	DNA · DNA perfect match	TCGACTATGCAT AGCTGATACGTA	45	50
3·**6**	DNA · CHIM perfect match	TCGACTA*TGCAT* AGCTGATACGTA	40	60
4·**8**	DNA · CHIM perfect match	TCGA**G**TA*TGCAT* AGCT**C**ATACGTA	38	60
4·**6**	DNA · CHIM mismatch in DNA	TCGA**G**TA*TGCAT* AGCTGATACGTA	no transition	–
3·**8**	DNA · CHIM mismatch in DNA	TCGACTA*TGCAT* AGCT**C**ATACGTA	no transition	–
3·**7**	DNA · CHIM mismatch in PNA	TCGACTA*TGCAT* AGCTGATAC**C**TA	35	18
5·**7**	DNA · DNA mismatch	TCGACTATGCAT AGCTGATAC**C**TA	35	18
3·**9**	Control, no complementary	TCGACTA*TGCAT* GCTGTACAAGTA	no transition	–
4·**9**	Control, no complementary	TCGA**G**TA*TGCAT* GCTGTACAAGTA	no transition	–
5·**9**	Control, no complementary	TCGACTATGCAT GCTGTACAAGTA	no transition	–

For example, mismatches in PNA complexes have been reported to lower the melting temperature of duplexes by 8–20°, twice that observed for mismatches in DNA · DNA duplexes [14]. Melting temperatures of PNA–DNA chimeras depend on various factors such as the DNA/PNA ratio in the chimera, sequence, and the position of the

linker molecule between DNA and PNA [16]. Our results show that, using PNA–DNA chimeras, it is possible to select a combination of conditions that eliminate hybridization with sequences carrying one single mismatch. We believe that these results will be of interest for mismatch detection in gene analysis by using DNA microarrays [11][12].

Conclusions. – In this study, PNA and PNA–DNA chimeras carrying thiol groups were used for surface functionalization of Au nanoparticles. We showed that citrate-stabilized Au nanoparticles can be successfully functionalized with PNA–DNA chimeras and remain stable after functionalization. The hybridization and melting properties of complexes formed from chimera–nanoparticle conjugates and oligonucleotide–nanoparticle conjugates are described for the first time. Similar to oligonucleotide–gold nanoparticle conjugates, conjugates with PNA–DNA chimeras gave sharper and more-defined melting profiles than those obtained for unmodified oligonucleotides. In addition, mismatch discrimination was more efficient than with unmodified oligonucleotides.

This work was supported by the *Comission of the European Union* as part of the *Information Societies Technology Programme* (IST-1999-11974), by the *Dirección General de Investigación Científica* (BQU2003-0397 and BFU2004-02048) and *The Generalitat de Catalunya* (2001-SGR-0049). We thank *Elisenda Ferrer* for her help on the preparation of PNA–DNA chimeras.

Experimental Part

General. Phosphoramidites and ancillary reagents used during oligonucleotide synthesis were from *Applied Biosystems* (USA), *Cruachem Ltd.* (Scotland), and *Glen Research* (USA). PNA Monomers protected with the Boc group were from *Applied Biosystems* (USA). Amino acid derivatives were from *Bachem* (Switzerland) and *Novabiochem* (Switzerland). The rest of the chemicals were purchased from *Aldrich*, *Sigma*, or *Fluka*. Long-chain-alkyl amino controlled-pore glass (LCA-CPG) was purchased from *CPG Inc.* (USA). Amino–polyethyleneglycol–polystyrene (PEG–PS) was purchased from *PerSeptive* (now *Applied Biosystems* USA). Methylbenzhydrylamine–polystyrene support was from *Novabiochem* (Switzerland). Solvents were from *S.D.S.* (France). Gold nanoparticles (13 nm, citrate-stabilized) were prepared as described elsewhere [7]. DNA synthesis was performed on a *392-Applied Biosystems* (USA) DNA synthesizer. UV/VIS Spectra: *UV-2103PC* and *Agilent-8453* spectrophotometers. Mass spectra: matrix-assisted laser-desorption-ionization time-of-flight (MALDI-TOF) MS were provided by the mass spectrometry service at the University of Barcelona.

Peptide Nucleic Acids. PNA Oligomer synthesis was carried out manually on a methylbenzhydrylamine(MBHA)–polystyrene support (5-μmol scale), following the synthesis cycle for the Boc/Z strategy described elsewhere [22]. The PNA monomers were added manually with a 5-molar excess, activated by *O*-(7-azabenzotriazol-1-yl)-1,1,3,3-tetramethyluronium hexafluorophosphate (HATU) and diisopropylethylamine ($^{i}Pr_2EtN$). The coupling reaction was monitorized by the ninhydrin test [23], and the absence of color in the soln. or resin beads indicated nearly quantitative yields (>95%). For the introduction of cysteine, Boc-Cys (Boc = (*tert*-butoxy)carbonyl) protected with the 4-methoxybenzoyl group was used. The Fm (= 9*H*-fluoren-9-yl)methyl) group was used for the protection of the γ-carboxylic group of glutamic acid. The last amino group was acetylated with Ac_2O and $^{i}Pr_2EtN$. After the completion of the sequence **2**, the Fm group was removed with piperidine, and the resulting support was treated with a mixture of CF_3COOH and CF_3SO_3H (by using Me_2S and *m*-cresol (= 3-methylphenol) as scavengers) as described [22]. The support from the synthesis of sequence **1** was treated directly with CF_3COOH/CF_3SO_3H and the scavengers. The resulting products were precipitated with Et_2O, and the residue was desalted with a *Sephadex G-25* column (*NAP-10*, *Pharmacia*, Sweden). The PNA-containing fractions were further purified by reversed-phase HPLC (*Nucleosil 120 C_{18}*, (250 × 8 mm); flow rate 3 ml/min; 25-min gradient from 0% *B* to 50% *B:* soln. *A* 5% MeCN in 0.1% CF_3COOH in H_2O; soln. *B:* 70% MeCN in 0.1% CF_3COOH in H_2O): desired PNA oligomer. MS: confirmation of the attribution of the major HPLC peak to the desired product. MALDI-TOF of **1**: 3306.9 ($[M+H]^+$; $C_{131}H_{168}N_{66}O_{38}S^+$; calc. 3306.7). MALDI-TOF of **2**: 3814.1 ($[M+Na]^+$; $C_{150}H_{194}N_{70}O_{49}S^+$; calc. 3793.1).

PNA – DNA Chimeras and Oligonucleotides. The 5′-thiolated oligonucleotides were prepared with standard (benzoyl- or isobutyryl-protected) 3′-(2′-cyanoethyl phosphoramidites) and the phosphoramidite of [$(MeO)_2$Tr]-protected 6-hydroxyhexyl disulfide (*Glen Research*, USA).

PNA – DNA chimeras were synthesized on a MeOTrNH – hexyl – succinate – NH – PEG – PS support as described in [24]. PNA Monomers were prepared as described [28]. PNA Sequence *TGCAT*-CONH-hexyl-OH was synthesized on a 10-μmol scale in a syringe equipped with a filter. The PNA monomers, in a 5-molar excess, were added manually. PNA-Monomer coupling was carried out, adding equal amounts of three solns.: *a*) 0.2M PNA monomer in MeCN (T, G, A) or 0.1M of the C monomer in CH_2Cl_2 (C), *b*) 0.2M HATU in MeCN and *c*) 0.2M $^{i}Pr_2EtN$; in MeCN; coupling time 15 min. After coupling, a capping with Ac_2O and 1-methyl-1*H*-imidazole was performed with the capping solns. from oligonucleotide synthesis and a capping time of 1 min. Deprotection of the MeOTrNH groups was carried out with 3% CCl_3COOH in CH_2Cl_2 (10×1 ml, 5 min) followed by thorough washing with MeCN, neutralization with 0.3M $^{i}Pr_2EtN$ in MeCN and washing with MeCN. The last PNA monomer is a T-linker molecule carrying an OH protected with the MeOTr group [25][27][28]. The oligonucleotide part was assembled on an automatic DNA synthesizer with standard 2-cyanoethyl phosphoramidites and following standard protocols (1-μmol scale). To characterize the PNA support, a short sequence of a DNA – PNA chimera was prepared (5′-TGCAGCC*TGCAT* – CONH – hexyl – OH-3) and purified by HPLC giving a major product that had the expected molecular mass. Electrospray-MS of 5′-TGCAGCC*TGCAT* – CONH – hexyl – OH-3′: 3611.0 (M^+, $C_{127}H_{166}N_{53}O_{60}P_7^+$; calc. 3611.4).

The resulting supports were treated with 1 ml of conc. ammonia (overnight, 55°). Supports carrying oligonucleotides and PNA – DNA chimeras with a thiol group at the 5′-end were treated overnight with 1 ml of 50 mM dithio-DL-threitol (DTT) in conc. ammonia at 55°. The excess of DTT was eliminated with a *Sephadex G-25* column (*NAP-10*, *Pharmacia*, Sweden) just prior to conjugation with Au nanoparticles.

Dithiol linkages in thiolated oligonucleotide solns. were cleaved prior to use by adding an appropriate amount of 0.1M dithiothreitol (DTT) in 0.17M sodium phosphate buffer (pH 8). Typically, 20 μl of DTT soln. was added to 100 μl of a 100 pmol/ml soln. of the oligonucleotide. The soln. was allowed to stand at r.t. for 0.5 h. The thiolated oligonucleotides were then desalted on a *NAP-10* (*Pharmacia*) column with 10 mM phosphate buffer (pH 7) as solvent. The optical absorbance at 260 nm of the purified oligonucleotide was used in conjunction with the known extinction coefficient of the oligonucleotide to determine the oligonucleotide concentration according to *Beer*'s law. Oligonucleotides were prepared for hybridization experiments by dissolving them at appropriate concentration in buffer soln. (0.3M NaCl, 10 mM phosphate buffer, pH 7).

Oligonucleotide – Gold Conjugates. Solns. of Au nanoparticles and oligonucleotides were mixed in appropriate amounts [29], *i.e.*, 2.63 nmol of oligonucleotide was used per ml of Au nanoparticles (the concentration of nanoparticles was 15.66 nM). The entire soln. was then brought to 10 mM sodium phosphate buffer (pH 7). The amounts of reagents used in each conjugate synthesis included a 1.5-molar excess of oligonucleotide. After 24 h, solns. were brought to 0.1M NaCl by addition of the appropriate amount of a 1M NaCl, 10 mM sodium phosphate buffer (pH 7) and allowed to stand at r.t. for a further 40 h. After this time, the solns. were centrifuged at 13200 r.p.m. for 30 min. The supernatant was removed, and the reddish solid at the bottom of the tubes was dispersed in 0.1M NaCl, 10 mM sodium phosphate buffer (pH 7) (the volume added was similar to that removed). This procedure was repeated, and the reddish solid at the bottom of the centrifuge tubes was dispersed in 0.3M NaCl, 10 mM sodium phosphate buffer (pH 7). Solns. were analyzed by UV/VIS spectroscopy, and absorbances at 260 and 520 nm were recorded. The concentration of the conjugate solns. were determined by using the absorbance of the soln. at 520 nm and *Beer*'s law [29]. Solns. were stored at r.t. Hybridization experiments were carried out by using 5-pmol amounts of each oligonucleotide – nanoparticle conjugate or chimera – nanoparticle conjugate (*i.e.*, 0.32 nmol of attached oligonucleotides) [30] in 0.3M NaCl, 10 mM phosphate buffer (pH 7) in a total reaction volume of 1 ml. The solns. were heated to 90° for 5 min, slowly cooled to r.t., and then left to hybridize for 24 h.

Hybridization Experiments. Oligonucleotide complexes were prepared by mixing 1 nmol of each strand in a total reaction volume of 1 ml. The solns. were then heated to 90° for 5 min, slowly cooled to r.t. and left to hybridize for 24 h. Oligonucleotide – nanoparticle complexes were prepared by mixing 5 pmol of each oligonucleotide – nanoparticle conjugate and chimera – nanoparticle conjugate in 0.3M NaCl, 10 mM sodium phosphate buffer (pH 7) in a total reaction volume of 1 ml. Hybridizations were also conducted in buffers containing 50 mM and 100 mM NaCl. The solns. were then heated to 90° for 5 min, allowed to cool to r.t. and left to hybridize for 24 h.

Melting Experiments. Optical melting curves were collected on a *Agilent-8453* spectrophotometer equipped with an *Agilent* temperature-controlling *Peltier* unit. The prehybridized soln. was transferred to a stoppered 1-cm-path-length cuvette and UV/VIS optical absorption spectra were recorded at 2° intervals, with a 1 – 2 min

heating time and a hold time of 1 min at each temp. interval, while the sample was heated from 20–90°. The data were collected as wavelength *vs.* absorbance spectra from which plots of absorbance *vs.* temp. at 260 nm were extracted. The melting temp. of each of the systems was determined from these graphs.

REFERENCES

[1] C. A. Mirkin, R. L. Letsinger, R. C. Mucic, J. J. Storhoff, *Nature (London)* **1996**, *382*, 607.
[2] A. P. Alivisatos, K. P. Johnsson, X. Peng, T. E. Wilson, C. J. Loweth, M. P. Bruchez, P. G. Schultz, *Nature (London)* **1996**, *382*, 609.
[3] R. C. Mucic, J. J. Storhoff, C. A. Mirkin, R. L. Letsinger, *J. Am. Chem. Soc.* **1998**, *120*, 12674.
[4] T. Taton, C. A. Mirkin, R. L. Letsinger, *J. Am. Chem. Soc.* **2000**, *122*, 6305.
[5] C. J. Loweth, W. B. Caldwell, X. Peng, A. P. Alivisatos, P. G. Schultz, *Angew. Chem., Int. Ed.* **1999**, *38*, 1808.
[6] R. Elghanian, J. J. Storhoff, R. C. Mucic, R. L. Letsinger, C. A. Mirkin, *Science (Washington, D.C.)* **1997**, *277*, 1078.
[7] J. J. Storhoff, R. Elghanian, R. C. Mucic, C. A. Mirkin, R. L. Letsinger, *J. Am. Chem. Soc.* **1998**, *120*, 1959.
[8] R. A. Reynolds, C. A., Mirkin, R. L. Letsinger, *J. Am. Chem. Soc.* **2000**, *122*, 3795.
[9] J. J. Storhoff, C. A. Mirkin, *Chem. Rev.* **1999**, *99*, 1849.
[10] S. J. Park, A. A. Lazarides, C. A. Mirkin, P. W. Brazis, C. R. Kannewurf, R. L. Letsinger, *Angew. Chem., Int. Ed.* **2000**, *39*, 3845.
[11] J. J. Storhoff, S. S. Marla, P. Bao, S. Hagenow, H. Mehta, A. Lucas, V. Garimella, T. Patno, W. Buckingham, W. Cork, U. R. Müller, *Biosens. Biotelectron*. **2004**, *19*, 875.
[12] J. J. Storhoff, A. D. Lucas, V. Garimella, Y. P. Bao, U. R. Müller, *Nat. Biotechnol.* **2004**, *22*, 883.
[13] P. E. Nielsen, M. Egholm, B. H. Berg, O. Buchardt, *Science (Washington, D.C.)* **1991**, *254*, 1497.
[14] M. Egholm, O. Buchardt, L. Christensen, C. Behrens, S. M. Freir, D. A. Driver, R. H. Bergh, S. K. Kim, D. Norden, P. E. Nielsen, *Nature (London)* **1993**, *365*, 566.
[15] B. Hyrup, P. E. Nielsen, *Biorg. Med. Chem*. **1996**, *4*, 5.
[16] E. Uhlmann, A. Peyman, G. Breipohl, D. W. Will, *Angew. Chem., Int. Ed*. **1998**, *37*, 2797.
[17] K. A. Williams, P. T. M. Veenhuizen, B. G. de la Torre, R. Eritja, C. Dekker, *Nature (London)* **2002**, *420*, 761.
[18] C. Coester, J. Kreuter, H. von Brisen, K. Langer, *Int. J. Pharm*. **2000**, *196*, 147.
[19] K. Langer, C. Coester, C. Weber, H. von Briesen, J. Kreuter, *Eur. J. Pharm. Biopharm*. **2000**, *49*, 303.
[20] R. Hölzel, N. Gajovic-Eichelmann, F. F. Bier, *Biosens. Bioelectron*. **2003**, *18*, 555.
[21] R. Chakrabarti, A. M. Klibanov, *J. Am. Chem. Soc*. **2003**, *125*, 12531.
[22] T. Koch, in 'Peptide Nucleic Acids. Protocols and Applications', Eds. P. E. Nielsen and M. Egholm, Horizon Scientific Press, 1999, p. 21.
[23] V. K. Sarin, S. B. Kent, J. P. Tam, R. B. Merrifield, *Anal. Biochem.* **1981**, *117*, 147.
[24] G. Breipohl, D. W. Will, A. Peyman, E. Uhlmann, *Tetrahedron* **1997**, *53*, 14671.
[25] P. J. Finn, N. J. Gibson, R. Fallon, A. Hamilton, T. Brown, *Nucleic Acids Res.* **1996**, *24*, 3357.
[26] A. C. van der Laan, R. Brill, R. G. Kuimelis, E. Kuyl-Yeheskiely, J. H. van Boom, A. Andrus, R. Vinayak, *Tetrahedron Lett.* **1997**, *38*, 2249.
[27] K. H. Petersen, D. K. Jensen, M. Egholm, P. E. Nielsen, O. Buchardt, *Bioorg. Med. Chem. Lett.* **1995**, *5*, 1119.
[28] E. Ferrer, M. Eisenhut, R. Eritja, *Lett. Pept. Sci*. **1999**, *6*, 209.
[29] T. A. Taton, in 'Current Protocols in Nucleic Acid Chemistry', John Wiley & Sons, Inc., New York, 2002, Chapt. 12.2.1–12.2.11.
[30] L. M. Demers, C. A. Mirkin, R. C. Mucic, R. A. Reynolds, R. L. Letsinger, R. Elghanian, G. Viswanadham, *Anal. Chem.* **2000**, *72*, 5535.

Received July 13, 2004